Communication

Nuclear Modification Factor of Inclusive Charged Particles in Au+Au Collisions at $\sqrt{s_{NN}} = 27$ GeV with the STAR Experiment

Alisher Aitbayev [1,2] **on behalf of STAR Collaboration**

1   Joint Institute for Nuclear Research (JINR), Joliot-Curie 20, Dubna 141980, Russia; a.ali.970424@gmail.com
2   Faculty of Physics and Technology, Al-Farabi Kazakh National University, Almaty 050040, Kazakhstan

Abstract: The Beam Energy Scan (BES) program at RHIC aims to explore the QCD phase diagram, including the search for the evidence of the 1st order phase transition from hadronic matter to Quark-Gluon Plasma (QGP) and the location of the QCD critical point. One of the features previously observed in the study of QGP is the effect of suppression of particle production with high transverse momenta p_T (>2 GeV/c) at energies $\sqrt{s_{NN}}$ = 62.4 − 200 GeV, which was deduced from the charged-particle nuclear modification factor (R_{CP}) measured using the data from Beam Energy Scan Program Phase I (BES-I) of STAR experiment. In 2018, STAR has collected over 500 million events from $Au+Au$ collisions at $\sqrt{s_{NN}}$ = 27 GeV as a part of the STAR BES-II program, which is about a factor of 10 higher than BES-I 27 GeV data size. In this report, we present new measurements of charged particle production and the nuclear modification factor R_{CP}, from this new 27 GeV data set and compare them with the BES-I results. The new measurements extend the previous BES-I results to higher transverse momentum range, which allows better exploration of the jet quenching effects at low RHIC energies, and may help to understand the effects of the formation and properties of QGP at these energies.

Keywords: heavy ion collisions; QCD phase transition; charged particle production; nuclear modification

1. Introduction

Collisions of heavy ions at high energies create a dense, strongly interacting, deconfined partonic fluid called quark-gluon plasma (QGP) [1–6]. Quantifying the properties of QGP is necessary for the description of the Quantum ChromoDynamics (QCD) phase diagram [7], as well as constraining parameters in cosmological models that describe the evolution of the universe through the QCD phase diagram [8]. The most common way to characterize the QCD phase diagram in heavy-ion experiments [9] is in the temperature (T) and baryon chemical potential plane [10]. High collision energies correspond to low initial baryon chemical potentials (μ_B), while low collision energies lead to high values of μ_B [11]. The crossover behavior at low μ_B region is predicted by Lattice QCD (LQCD) calculations [12,13], while a first-order phase transition is predicted at sufficiently large μ_B [14,15], which would imply the existence of the critical end-point.

To experimentally study the phase structure of QCD matter as a function of T and μ_B, the Relativistic Heavy Ion Collider (RHIC) has launched the Beam Energy Scan (BES) program. The essence of the program is to carry out collisions at different energies, thereby creating systems with different initial conditions of T and μ_B to search for the critical point of the phase diagram. The graph in Figure 1 shows the QCD phase diagram with mapping of the available experimental areas reached at different collision energies during all phases of the BES program. By creating diverse initial states, we aim to achieve the intersection of different reaction trajectories with the phase boundary at various values of T and μ_B. This will allow us to explore interesting features of the phase diagram, including the conjectured critical point and the first-order phase transition.
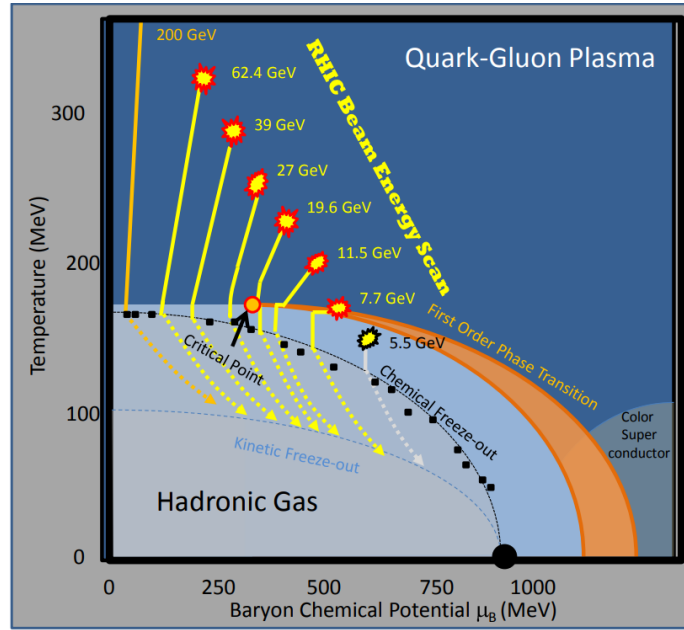
Figure 1. The picture of the QCD Phase Diagram with marked coverage of the RHIC BES program. Yellow trajectories represent schematics of the collision evolution at different energies of the BES program. The red circle symbolizes the critical point. Note, that yellow lines and the red circle are for illustrative purpose only [1].

The suppression effect of charged particle production with high transverse momenta ($p_T > 2$ GeV/c) is one of the most interesting results observed at the Solenoidal Tracker At RHIC (STAR) experiment during the BES-I program. This effect has been interpreted as the increase in energy loss of partons in the quark-gluon plasma produced at high energy heavy ion-collisions. It is commonly referred to as jet quenching in dense partonic matter [16,17] and was predicted as a sign of the formation of the QGP phase, where simple model of hadron scattering cannot describe the observations. This effect can be quantified using the nuclear modification factor R_{CP}. The nuclear modification factor (R_{CP}) can be experimentally calculated as follows:

$$R_{CP} = \frac{\langle N_{coll} \rangle_{Peripheral}}{\langle N_{coll} \rangle_{Central}} \frac{\left(\frac{d^2 N}{dp_T d\eta} \right)_{Central}}{\left(\frac{d^2 N}{dp_T d\eta} \right)_{Peripheral}}. \tag{1}$$

In this context, $\langle N_{coll} \rangle$ denotes the mean number of binary collisions within a specific centrality class, and it can be approximated through the use of a Glauber Monte Carlo simulation [18]. If we consider heavy-ion collisions as a superposition of N_{coll} independent binary nucleon-nucleon collisions, the R_{CP} value would be equal to 1 across the entire transverse momentum (p_T) range. Effects that elevate the particle yield per binary collision in central heavy-ion collisions compared to $p + p$ or peripheral collisions are collectively referred to as enhancement effects, resulting in $R_{CP} > 1$. Conversely, those that diminish the particle yield are known as suppression effects, leading to $R_{CP} < 1$. Consequently, R_{CP} provides insight into whether enhancement or suppression effects dominate, although it does not quantify their magnitudes separately. Equation (1) compares the particle production at very small impact parameters (central class), where the mean path length through the produced nuclear medium might be longer, with that at very large impact parameters (peripheral class), where shorter in-medium path lengths should yield smaller energy loss [2].

Certain physical effects occurring in the nuclear medium after the collision can affect hadron production in specific kinematic ranges, effectively masking suppression due to jet quenching. The Cronin effect is one such phenomenon. In asymmetric collisions where

heavy nuclei collide the light one, the phenomenon of Cold Nuclear Matter (CNM) was first observed [19–21], where an increase in production of high p_T particles was measured instead of suppression. It was shown that the enhancement of the Cronin effect increases as the impact parameter decreases [22,23]. Additionally, other processes in heavy-ion collisions, such as radial flow and particle coalescence, can induce enhancement [24]. In radial flow, the transition of particles from low p_T to higher momenta in central events, along with the formation of p_T-ridges or coalescence, overall leads to an increase in the nuclear modification factor (R_{CP}). In a nuclear collision, there is an interplay of above-mentioned effects and jet quenching which shifts high-p_T particles towards lower momenta will lead to the measured results.

Therefore, observing a nuclear modification factor exceeding unity does not automatically imply the absence of quark-gluon plasma formation. Resolving these competing effects can be accomplished using additional methods, such as event-plane-dependent nuclear modification factors [2]. Figure 2 illustrates the nuclear modification factor measured for inclusive charged hadrons produced in *Au+Au* collisions during the BES-I program [2]. At high transverse momenta ($p_T > 2 GeV/c$), there is a gradual transition from strong enhancement to strong suppression with increasing collision energies.
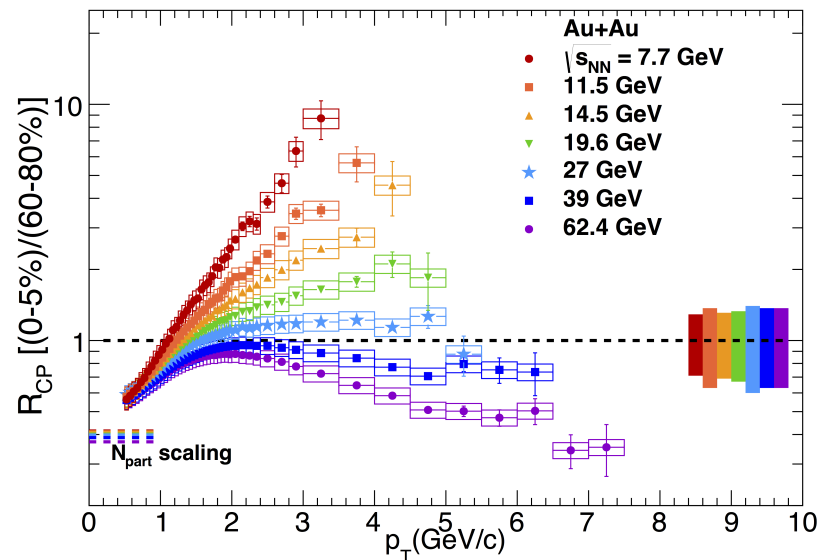

Figure 2. Unidentified charged hadron R_{CP} for RHIC BES-I and high energy data. The uncertainty bands at unity on the right side of the plot correspond to the p_T independent uncertainty in N_{coll} scaling with the color in the band corresponding to the color of the data points for that energy. The vertical uncertainty bars correspond to statistical uncertainties and the boxes to systematic uncertainties [2].

In this report, preliminary results of the nuclear modification factor for *Au+Au* collisions at collision energy of $\sqrt{s_{NN}}$ = 27 GeV from the STAR BES-II program will be presented.

2. Data Analysis

The data under analysis was collected in 2018 from *Au+Au* collisions at a center-of-mass energy of $\sqrt{s_{NN}} = 27$ GeV during the BES-II at RHIC runs by the STAR detector. The TPC and TOF subsystems of STAR provide tracking and particle identification for our analysis. To measure momentum, these detectors operate in a magnetic field with an intensity of 0.5 T, allowing the trajectory of passing charged particles to be bent. In combination with the path length of trajectories measured in the TPC and the time of flight from the TOF, this provides information on the speed of charged particles, denoted as β c, which is used for particle identification. $1/\beta$ is determined as $\sqrt{(\frac{mc}{p})^2 + 1}$, where *m* is

the particle mass, p is the particle momentum, and c is the time of flight. Centrality is determined by the charge particle multiplicity at mid-rapidity in the TPC. Events at low energies caused by ion interactions with the beam pipe were excluded by introducing a restriction along the XY plane ($V_r = \sqrt{V_x^2 + V_y^2} < 2cm$). Additionally, only events within a range of 75 cm (-75; 75 cm) along the Z axis were selected to consider only particles formed at the central region of the detector. To reduce the contribution of particles from secondary interactions and weak decays, only tracks with a distance of closest approach (DCA) from the primary vertex of less than 2 cm were chosen. We require tracks to fall in the pseudorapidity range $|\eta| < 1$ to ensure that all selected tracks pass entirely through the central part of the TPC. The parameter nHitsFit represents the number of hits that can be used to reconstruct a track. Increasing the number of hits in a track improves momentum resolution, but requiring a very large number of hits reduces the quality of tracks with low transverse momentum p_T values. The study findings underscore the significance of having a minimum of 16 hits for robust analysis, alongside emphasizing that the ratio of points utilized in track reconstruction to the total available points (nFitOverPoss) should exceed 0.52 to prevent track fragmentation. In assessing p_T and tracking efficacy within the TPC, Monte Carlo particle tracks calibrated using GEANT-3 were employed. This was followed by STAR detector simulations and the integration of generated signals into real events across varying energy levels and centralities. Subsequently, the efficiency of charged hadron tracking was computed as a weighted mean of fits to individual particle efficiency, weighted by the analysis of adjusted spectra. This approach facilitated the extrapolation of charged hadron tracking efficiency to higher p_T values compared to what could be derived from singular particle spectra. Moreover, the efficiency remains stable as p_T escalates within the extrapolation domain, thus mitigating the influence of extrapolation on systemic uncertainties.

The systematic errors were calculated by varying the selection criteria. The analysis cuts used to estimate systematic uncertainties are listed in Table 1.

Table 1. The default and changed values of event and track cuts for systematic uncertainties measurement.

Systematic sources	Default	Variation(s)
r_vtx	2	1–3 [cm]
z_vtx	75	65–70 [cm]
DCA	2	1.5–2.5 [cm]
nHitsFit	16	12–20
nFitOverPoss	0.5	0.6

3. Results and Discussion

The transverse momentum particle spectra for $Au+Au$ collisions at energy of $\sqrt{s_{NN}} = 27$ GeV for inclusive charged particles in different centrality classes are shown in Figure 3.

The spectra are shown for six centrality classes, where the upper spectrum corresponds to 0–5% centrality and the spectra below for more peripheral collisions in decreasing order. Each set of data was mutliplied by a power of 10 for better visibility.

From Figure 3, it can be noticed that in the BES-II program, the spectra have a greater coverage in terms of transverse momentum p_T for all centrality classes, which enables a more comprehensive investigation of the nuclear modification factor.
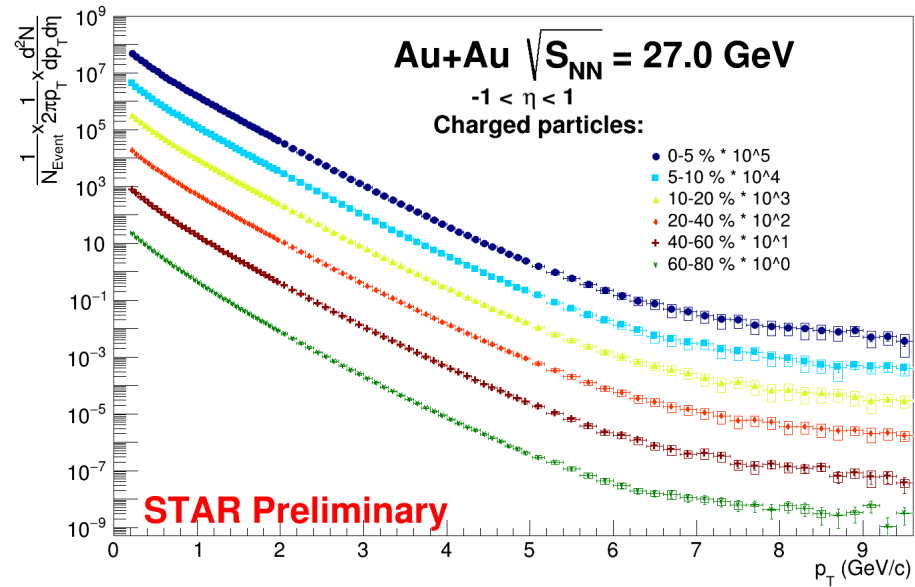
Figure 3. Transverse momentum distribution of inclusive charged particles for collision energy of 27 GeV. Each spectrum corresponds to a certain centrality class and is multiplied by coefficient from $1–10^5$ for visibility. The vertical error bars correspond to statistical uncertainties and the colored boxes to the systematic uncertainties.

Figure 4 demonstrates the R_{CP} for $Au+Au$ collisions at a collision energy of 27 GeV, for the pseudorapidity range of $-1 < \eta < 1$. The R_{CP} was calculated as:

$$R_{CP} = \frac{\langle N_{coll} \rangle_{Peripheral}}{\langle N_{coll} \rangle_{Central}} \frac{d^2N/dp_T d\eta_{0-5\%}}{d^2N/dp_T d\eta_{60-80\%}}. \tag{2}$$

The vertical lines and horizontal lines in Figure 4 represent the statistical errors and bin widths, respectively and the colored boxes the systematic uncertainties, while the error band at unity on the right side of the plot corresponds to the p_T independent uncertainty on N_{coll} scaling. In Figure 2, depicting R_{CP} for energy collision 27 GeV with a transverse momentum ranging from 5.5 to 6 GeV/c, it's evident that R_{CP} falls below 1. This discrepancy contrasts with my preceding analysis, where R_{CP} exceeded 1. The variance is attributable to the influence of pseudo-rapidity on R_{CP}. Specifically, in my analysis, pseudo-rapidity is set at 1, whereas in the previous one, it stood at 0.5.

A growth of R_{CP} can be observed at low values of p_T (up to $p_T \approx 2$ GeV/c), which is affected by effects such as Cronin enhancement [19–21], radial flow [24], and the relative dominance of coalescence over fragmentation during hadronization [24]. However, as p_T increases, R_{CP} reaches a plateau and then demonstrates suppression of hadrons produced in central collisions with respect to peripheral collisions.
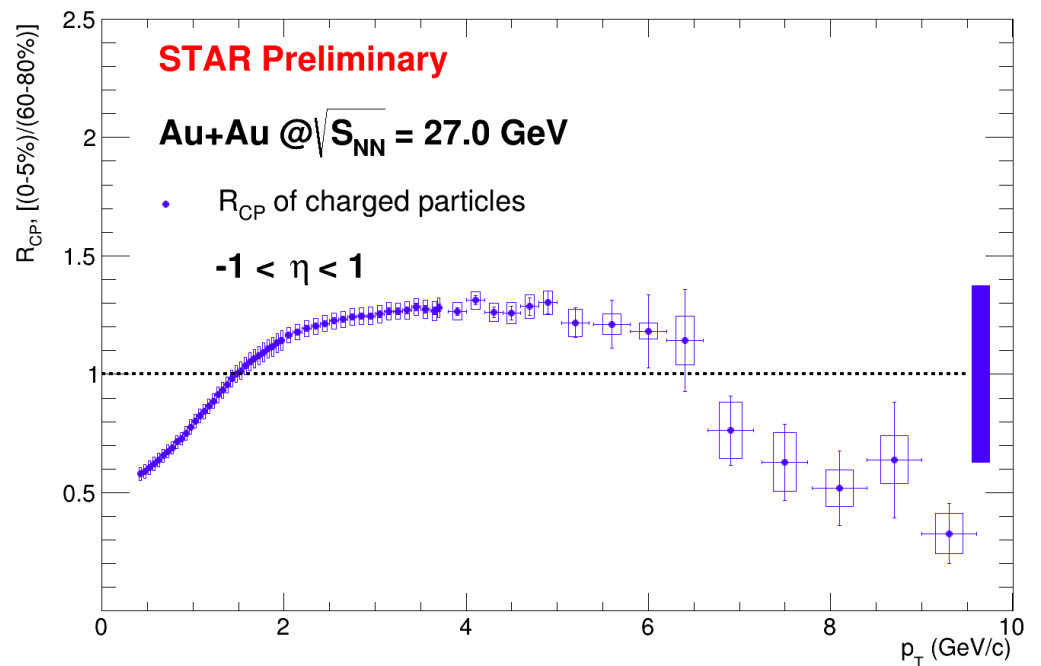
Figure 4. R_{CP} for inclusive charged particles at $\sqrt{s_{NN}} = 27$ GeV collision energy. The error band at unity on the right side of the plot corresponds to the p_T independent uncertainty on N_{coll} scaling. The vertical error bars correspond to statistical uncertainties and the colored boxes to the point-to-point systematic uncertainties.

4. Conclusions

In this report, the nuclear modification factor R_{CP} for $Au+Au$ collisions at a collision energy of $\sqrt{s_{NN}} = 27$ GeV at the STAR experiment was presented. A significant extension to higher p_T values has been achieved compared to the Rcp observed in program BES-I. This advancement has enabled a more accurate characterization of the behavior of the nuclear modification in medium. Notably, suppression of particle production at high p_T is observed. However, the data is not sufficient to claim the formation of QGP based on this observable, and further study and investigation of the behavior of the nuclear modification factor dependence on energy on the data from STAR BES-II program are necessary. Future comparisons with hydrodynamic model with the propagation of non-equilibrium high-energy jet approach may help interpret the presented data.

Data Availability Statement: All the data used in this article is already included in the article.

Conflicts of Interest: The authors declare no conflict of interest.

Abbreviations

The following abbreviations are used in this manuscript:

QCD	Quantum ChromoDynamics
QGP	Quark-Gluon Plasma
BES	Beam Energy Scan
BES-I	Beam Energy Scan Program Phase I
BES-II	Beam Energy Scan Program Phase II
LQCD	Lattice Quantum ChromoDynamics
R_{CP}	Nuclear Modification Factor

References

1. Odyniec, G. The RHIC Beam Energy Scan program in STAR and what's next ... *J. Phys. Conf. Ser.* **2013**, *455*, 012037 [CrossRef]
2. Adamczyk, L. et al. [STAR Collaboration] Beam Energy Dependence of Jet-Quenching Effects in Au+Au Collisions at $\sqrt{s_{NN}}$ = 7.7, 11.5, 14.5, 19.6, 27, 39, and 62.4 GeV. *Phys. Rev. Lett.* **2018**, *121*, 032301. [CrossRef]
3. Arsene, I. et al. [BRAHMS Collaboration] Quark gluon plasma and color glass condensate at RHIC? The Perspective from the BRAHMS experiment. *Nucl. Phys. A* **2005**, *757*, 1–27. [CrossRef]
4. Back, B.B. et al. [PHOBOS Collaboration] The PHOBOS perspective on discoveries at RHIC. *Nucl. Phys. A* **2005**, *757*, 28–101. [CrossRef]
5. Adams, J. et al. [STAR Collaboration] Experimental and theoretical challenges in the search for the quark gluon plasma: The STAR Collaboration's critical assessment of the evidence from RHIC collisions. *Nucl. Phys. A* **2005**, *757*, 102–183. [CrossRef]
6. Adcox, K. et al. [PHENIX Collaboration] Formation of dense partonic matter in relativistic nucleus-nucleus collisions at RHIC: Experimental evaluation by the PHENIX collaboration. *Nucl. Phys. A* **2005**, *757*, 184–283. [CrossRef]
7. Gyulassy, M.; McLerran, L. New forms of QCD matter discovered at RHIC. *Nucl. Phys. A* **2005**, *750*, 30–63. [CrossRef]
8. McInnes, B. Trajectory of the cosmic plasma through the quark matter phase diagram. *Phys. Rev. D* **2016**, *93*, 043544. [CrossRef]
9. Laermann, E.; Philipsen, O. The Status of lattice QCD at finite temperature. *Ann. Rev. Nucl. Part Sci.* **2003**, *53*, 163–198. [CrossRef]
10. Fukushima, K.; Hatsuda, T. The phase diagram of dense QCD. *Rept. Prog. Phys.* **2011**, *74*, 014001. [CrossRef]
11. Cleymans, J.; Oeschler, H.; Redlich, K.; Wheaton, S. Comparison of chemical freeze-out criteria in heavy-ion collisions. *Phys. Rev. C* **2006**, *73*, 034905. [CrossRef]
12. Aoki, Y.; Endrodi, G.; Fodor, Z.; Katz, S.D.; Szabo, K.K. The Order of the quantum chromodynamics transition predicted by the standard model of particle physics. *Nature* **2006**, *443*, 675–678. [CrossRef]
13. Bazavov, A. et al. [HotQCD Collaboration] Chiral crossover in QCD at zero and non-zero chemical potentials. *Phys. Lett. B* **2019**, *795*, 15–21. [CrossRef]
14. Bowman, E.S.; Kapusta, J.I. Critical Points in the Linear Sigma Model with Quarks. *Phys. Rev. C* **2009**, *79*, 015202. [CrossRef]
15. Ejiri, S. Canonical partition function and finite density phase transition in lattice QCD. *Phys. Rev. D* **2008**, *78*, 074507. [CrossRef]
16. Bjorken, J.D. Energy Loss of Energetic Partons in Quark-Gluon Plasma: Possible Extinction of High p_T Jets in Hadron-Hadron Collisions. FERMILAB-PUB-82-059-THY, FERMILAB-PUB-82-059-T. 1982. Available online: https://cds.cern.ch/record/141477 (accessed on 8 January 2024).
17. Gyulassy, M.; Levai, P.; Vitev, I. Jet quenching in thin quark gluon plasmas. 1. Formalism. *Nucl. Phys. B* **2000**, *571*, 197–233. [CrossRef]
18. Miller, M.L.; Reygers, K.; Sanders, S.J.; Steinberg, P. Glauber modeling in high energy nuclear collisions. *Ann. Rev. Nucl. Part. Sci.* **2007**, *57*, 205–243. [CrossRef]
19. Cronin, J.W.; Frisch, H.J.; Shochet, M.J.; Boymond, J.P.; Mermod, R.; Piroue, P.A.; Sumner, R.L. Production of hadrons with large transverse momentum at 200, 300, and 400 GeV. *Phys. Rev. D* **1975**, *11*, 3105–3123. [CrossRef]
20. Antreasyan, D.; Cronin, J.W.; Frisch, H.J.; Shochet, M.J.; Kluberg, L.; Piroue, P.A.; Sumner, R.L. Production of Hadrons at Large Transverse Momentum in 200-GeV, 300-GeV and 400-GeV p p and p n Collisions. *Phys. Rev. D* **1979**, *19*, 764–778. [CrossRef]
21. Straub, P.B.; Jaffe, D.E.; Glass, H.D.; Adams, M.R.; Brown, C.N.; Charpak, G.; Cooper, W.E.; Crittenden, J.A.; Finley, D.A.; Gray, R.; et al. Nuclear dependence of high-x_t hadron and high-τ hadron-pair production in p-A interactions at $\sqrt{s}$ =38.8 GeV. *Phys. Rev. Lett.* **1992**, *68*, 452–455. [CrossRef] [PubMed]
22. Vitev, I. Initial state parton broadening and energy loss probed in d + Au at RHIC. *Phys. Lett. B* **2003**, *562*, 36–44. [CrossRef]
23. Accardi, A.; Gyulassy, M. Cronin effect and geometrical shadowing in d+Au collisions: pQCD versus colour glass condensate. *J. Phys. Nucl. Part. Phys.* **2004**, *30*, 5969. [CrossRef]
24. Greco, V.; Ko, C.M.; Levai, P. Parton coalescence at RHIC. *Phys. Rev. C* **2003**, *68*, 034904. [CrossRef]